Structure of InSb(001) surface

2010 J. Phys.: Condens. Matter 22 265001

(http://iopscience.iop.org/0953-8984/22/26/265001)

J. Phys.: Condens. Matter **22** (2010) 265001 (8pp) doi:10.1088/0953-8984/22/26/265001

Structure of InSb(001) surface

Dawid Toton[1,2], Jiangping He[1,3], Grzegorz Goryl[2], Jacek J Kolodziej[2], Szymon Godlewski[2], Lev Kantorovich[1] and Marek Szymonski[2]

[1] Department of Physics, King's College London, The Strand, London WC2R 2LS, UK
[2] Department of Physics of Nanostructures and Nanotechnology, Jagiellonian University, Reymonta 4, PL 30-059, Krakow, Poland
[3] Geography Department, King's College London, The Strand, London WC2R 2LS, UK

Received 22 February 2010, in final form 1 March 2010
Published 24 May 2010
Online at stacks.iop.org/JPhysCM/22/265001

Abstract
The InSb(001) surface has been studied experimentally, using room temperature scanning tunnelling microscopy (RT STM), and theoretically, using *ab initio* density functional theory (DFT) calculations. RT experimental STM images show bright lines running along the bulk crystal [110] direction. Resolved features between the bright lines whose appearance depends on the applied bias voltage confirm clearly the c(8 × 2) reconstruction of this surface. Our calculations, which are reported for this surface for the first time, include the reconstructed 4 × 2 and c(8 × 2) surfaces, the latter according to the so-called ζ-model proposed previously by Lee *et al* and Kumpf *et al*. A 'defective' structure proposed previously by Kumpf *et al*, which contains an extra In atom within a top bilayer is also considered. In all cases, we obtained stable structures. Calculated STM images for the c(8 × 2) reconstruction obtained using the Tersoff–Hamann approximation compare extremely well with the experimental ones. We also find that the defect structure may not be clearly visible in the STM images. Finally, a brief discussion is given on the other, although closely related, phase of the same surface observed previously in low temperature (LT) experimental STM images (Goryl *et al* 2007 *Surf. Sci.* **601** 3605).

(Some figures in this article are in colour only in the electronic version)

1. Introduction

$A_{III}B_V$ compounds are widely used in electronic and optoelectronic devices and as substrates for growing thin films. They have also been used in nanotechnology for molecular deposition and growth of nanostructures as templates because of the anisotropy of their surfaces due to usually quite complicated large-index reconstructions.

The InSb member of this family has the highest mobility and hence the promise to be used soon in microelectronics on a wide scale. In this paper we are interested in the (001) face of the InSb crystals, which display a number of interesting properties, such as e.g. formation of molecular wires [1, 2] and may be useful for nanotechnology applications. This surface is known for many $A_{III}B_V$ compounds to undergo a number of complex reconstructions depending on the preparation procedures, e.g. prevalence of one species over the other in surface–gas equilibrium [3]. The InSb(001) c(8 × 2) reconstruction is typically obtained by growth in B_V-deficient conditions or by ion sputtering and annealing under UHV. This reconstruction has been extensively studied and the corresponding so-called structural ζ-model has been proposed [4, 5]; this was later supported experimentally using both scanning tunnelling microscopy (STM) [6] and non-contact atomic force microscopy (NC-AFM) [7]. According to this model, the surface structure is dominated by the rows of In atoms running in the [110] direction. These may show in the room temperature (RT) STM images of this surface [6] as linear bright features (lines) forming on wide terraces as a 'ladder' like structure. The top bilayer in the surface has the (4 × 1) symmetry. However, because of the dimerization of In atoms in the second bilayer, the surface symmetry is actually lowered to that corresponding to the c(8 × 2) reconstruction. Note that somewhat different patterns in STM images can be obtained by changing the scanning conditions [6].

In spite of the fact that considerable theoretical effort has been made to investigate this and other reconstructions of some members of the $A_{III}B_V$ family of compounds, as far as we are aware, no theoretical calculations of the InSb(001)

c(8 × 2) reconstruction exist until now, so that the existing interpretation of the STM images taken so far [6] cannot be completely justified. For instance, one cannot be entirely convinced that the bright lines running in the [110] direction in the experimental images correspond to the so-called In-1 atoms of the Kumpf *et al* model [5]. Correspondingly, dim features running between the bright lines in the same direction in the STM images must also be interpreted on the atomic scale. These identifications are extremely important for purposes of e.g. nanotechnology in order to be sure that designed atomic and molecular structures can be built at desired locations on the surface.

The main purpose of this paper is to fill in this gap in the interpretation of the STM images and to confirm the Kumpf *et al* model [5]. For the first time, we present an extensive set of *ab initio* density functional theory (DFT) calculations of the (001) termination of the InSb surface. A number of possible structures are considered, including the one corresponding to the ζ-model, and their energies, geometries, and electronic properties, including the STM images, are discussed. In parallel, we also present new room temperature (RT) STM images of this surface obtained at different bias conditions. The theoretical calculations are found to agree remarkably well with the experimental data.

It must be noted that some additional features become apparent at low temperature (LT) STM images [6] taken at 77 K which seemingly break the RT c(8 × 2) reconstruction suggesting that at LT the symmetry of the surface is lower, i.e. the structure does not correspond exactly to the ζ-model anymore. The work on identifying this LT structure is in progress and is not addressed in this paper. However, at the end of the paper we provide a brief discussion of the LT phase and what modifications we expect are required in our model in order to explain it as well.

The plan of the paper is as follows. The section 2 starts with a brief summary of the experimental and theoretical methods used; in section 3 experimental results are summarized, while our DFT results on the surface structures studied are presented in section 4. Conclusions are made in section 5.

2. Method

2.1. Experimental details

The experiment is carried out in an ultra-high vacuum (UHV) system with a base pressure better than 10^{-10} mbar. The system allows for surface preparation, low energy electron diffraction (LEED) studies, and scanning tunnelling microscopy studies *in situ*. Epi-ready, undoped InSb wafers, mounted on tantalum plates are initially annealed in UHV, at 700 K, for several hours and then sputter-cleaned at the same temperature, using a rastered 700 eV Ar^+ ion beam, with an incidence angle 60° off-normal and a current density of 0.5–1.0 μA cm^{-2}. The sputtering cycles of 1 h duration are repeated until a clear c(8 × 2) LEED pattern is observed. Final thermal annealing to 700 K for 5 h is applied. Clean, crystalline surfaces are imaged in constant current mode, using an Omicron LT-STM microscope, at room temperature. Electrochemically etched tungsten tips are used as probes.

2.2. Theoretical

In our calculations we mostly used an *ab initio* SIESTA method [8], which is based on periodic boundary conditions and the method of pseudopotentials. We used the Perdew–Burke–Ernzerhof (PBE) [9] density functional and the double zeta polarized (DZP) numerical basis set corresponding to a confinement energy of 10 meV. All geometries were relaxed until the forces on the atoms were less then 0.04 eV Å^{-1}. The calculated lattice constant of the bulk InSb crystal (space group T_d^2, zinc blende structure) was found to be 6.66 Å (75 **k**-points and 400 Ryd were used for the Brillouin zone sampling and the real space mesh cutoff, respectively), which is within 3% accuracy of the experimental value of 6.4794 Å [10, 11].

To test the settings of the SIESTA calculations, we have also performed a number of plane wave calculations with the VASP code [12, 13]. The same density functional as in our SIESTA calculations was used. Using the PAW method to account for the core electrons [14], 21.98 Ryd for the plane wave cutoff and 11 × 11 × 11 Monkhorst–Pack **k**-points sampling, a result, very similar to the SIESTA lattice constant, of 6.64 Å was obtained.

The bulk calculations indicate that the SIESTA In and Sb pseudopotentials, as well as the localized basis set used, are sufficiently good for the purpose of this study.

When calculating STM images, we used the Tersoff–Hamann approximation [15] whereby the local electronic density of states (LDOS) serves as an approximation for the STM signal. The LDOS is obtained by integrating the Kohn–Sham states probabilities, $|\psi_\epsilon(\mathbf{x})|^2$, either over the energies $\epsilon_F - |eV| < \epsilon < \epsilon_F$ (occupied states or negative bias V) or $\epsilon_F < \epsilon < \epsilon_F + |eV|$ (unoccupied states, positive bias), ϵ_F being the Fermi energy of the system and e the electronic charge. This approximation is appropriate for small bias voltages and not very close tip–surface distances. Since the tip information does not enter the LDOS of the surface, the calculated STM images do not depend on the particular tip structure.

3. Room temperature STM measurements

Examples of room temperature STM patterns obtained on the InSb(001) surface are shown in figure 1 (right panels) for negative and positive bias voltages. At negative sample bias voltages (occupied states imaging) the typical pattern is characterized by: (i) continuous bright lines running in the [110] direction which are separated by four times the basic surface lattice unit $a = 4.58$ Å (i.e. by $4a = 18.32$ Å), and (ii) rows of rectangular features running between the lines which are repeated with the double unit period ($2a = 9.16$ Å). Importantly, the positions of the rectangular features on both sides of the bright lines are shifted (glide reflection symmetry), forming a brick-wall pattern and clearly confirming the c(8×2) reconstruction. Qualitatively similar patterns are observed for sample biases ranging from −0.7 to −2 V, the only differences between them are in a relative brightness of the

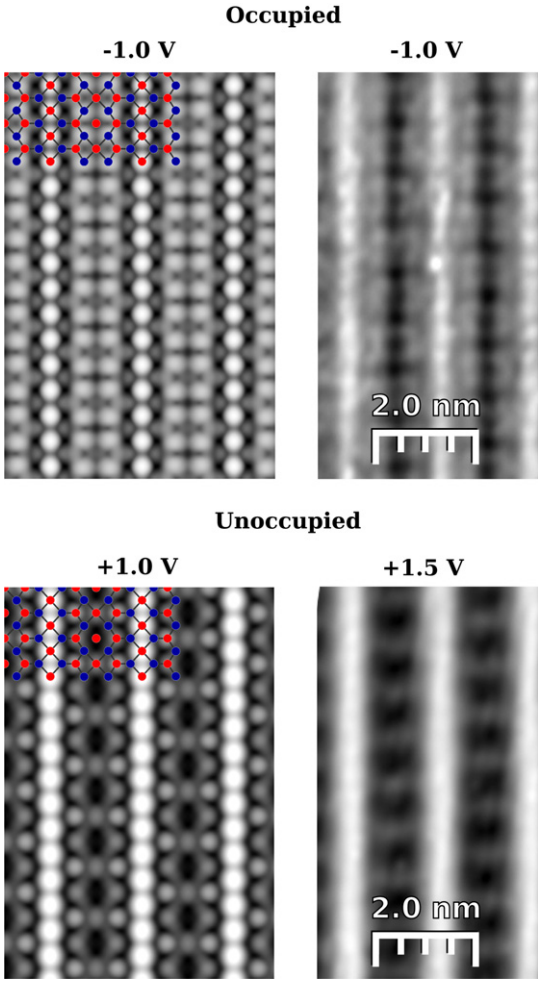

Figure 1. Calculated (left panels) and experimental room temperature (right panels) STM images of the c(8 × 2) reconstructed InSb(001) surface corresponding to occupied and unoccupied electronic states of the surface. The bias voltages are as indicated. Both experimental images were taken at the current of 10 pA. For convenience, the upper bilayer of atoms is superimposed on each calculated image with In atoms shown red/light grey and Sb atoms shown blue/dark grey.

continuous rows and the rectangular features. The positive bias (unoccupied states) STM image (the right-lower panel in figure 1) also displays continuous bright lines running in the same [110] direction. Since we have recorded STM frames where the bias voltage is reversed during the scan, it is evidenced that the continuous rows are imaged over the same atomic rows both for negative and positive sample bias voltages. Between the lines we see short parallel lines perpendicular to the [110] direction. These short lines are sometimes replaced by elongated oval features making a similar visual impression. These features are repeated with double unit period along the [110] direction. With a glide reflection axis found on the continuous row and the glide vector corresponding to a basic surface unit (4.58 Å), the empty state pattern has the clear c(8 × 2) symmetry as well. Similar empty states patterns are observed in a broad range of bias voltages from +0.75 to +2.0 V.

Although no detailed experimental STM study on the c(8 × 2) reconstructed InSb(001) surface is available in the literature (i.e. for a broad sample bias voltage range), some features reported earlier can be compared with our data. The old data recorded by Schweitzer *et al* [16] evidenced strongly dominating double rows running along the [110] direction with a single periodicity (equal to the a) along it. The pattern was recorded with a bias voltage of −3.0 V, which is beyond the range we have studied. Nevertheless, when going from −0.7 eV bias towards the −2.0 eV bias, we have seen a trend that the rectangular features decompose gradually into four round spots, effectively giving a double row similar to that reported in [16] already at the bias of −2.0 V. Also we have seen that the continuous row may be brighter or darker depending on the bias; it is not excluded that it may become completely invisible due to specific combinations of the bias and the tip structure. Other literature STM patterns are perfectly consistent with our data. These include the data by Varekamp *et al* [17] recorded at −1.9 V and the data by Davis *et al* [18] recorded at bias voltages of −2.0 and +1.1 V.

In order to characterize the observed features, *ab initio* density functional calculations (DFT) were conducted, as described in detail in the forthcoming sections.

4. DFT study of the InSb(001) c(8 × 2) reconstruction

In this section we describe our DFT calculations of the InSb(001) surface. Several structures are considered and all are shown to be stable minima. Then the STM images are reported and compared with experimental ones.

4.1. Relaxed geometries and energetics

The InSb(001) c(8 × 2) surface can be obtained from the 4 × 2 reconstruction by a shift along the [110] direction of several surface atoms ([4] and see below). Therefore, we first considered this reconstruction.

In all our SIESTA surface calculations the real space mesh cutoff of 200 Ryd was used. Typically, we used the 1 × 4 × 1 mesh of **k**-points due to a large supercell size (four points correspond to the direct space [110] direction). We checked that inclusion of more **k**-points changes atomic positions by no more than 0.01 Å. Two bottom layers of the slab, together with the terminating hydrogen atoms (see figure 2), were fixed, all other atoms were fully allowed to relax. To check the pseudopotentials, the basis set and other settings of our SIESTA calculations, the 4 × 2 surface was also relaxed using the VASP code with the plane wave cutoff of 22 Ryd and the 2 × 4 × 1 Monkhorst–Pack **k**-points sampling.

The relaxed supercell used in our calculations of the 4 × 2 reconstruction is shown on the left in figure 2 (both top and side views). It consists of two primitive unit cells. The slabs containing between 4 and 10 layers were considered with hydrogen atoms terminating the bottom layer; in all cases the hydrogen atoms were fixed as well the two bottom layers which were kept in the bulk positions. By analysing the surface energies of the slabs of different thickness, we find that a 4 layer slab was sufficient. However, to converge the vertical atomic positions of the upper layer atoms, which significantly affect the appearance of the calculated STM images, much bigger slabs are required. Therefore, the 10 layer slab was mostly used in this work.

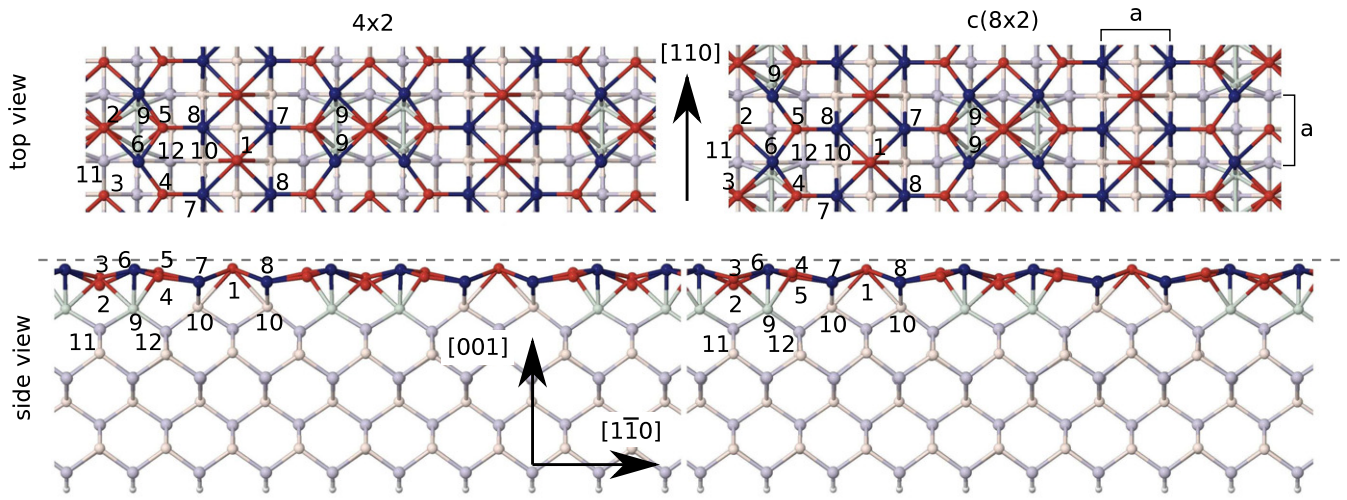

Figure 2. Two InSb(001) surfaces relaxed by SIESTA: 4 × 2 (left) and c(8 × 2) (right) reconstructions, the top (upper panels) and side (lower) views shown for convenience. In the case of the c(8 × 2) system, the actual primitive cell is two times smaller. The same system size is shown in the case of the 4 × 2 reconstruction for the ease of comparison with the other reconstruction. The bottom of the slabs are terminated by hydrogen atoms (shown white). In and Sb atoms of the upper layers are shown as red/mid grey and blue/dark grey circles, respectively, paler colours are used for atoms in deeper layers. The main atoms in the upper layers are numbered for convenience in accordance with [19, 5]. The [110] and [1$\bar{1}$0] directions are indicated, as well as the $z = 0$ plane (with the dashed line in the lower panels) chosen at the positions of the upper layer atoms if no reconstruction and relaxation have happened. The common unit length in the [110] and [1$\bar{1}$0] directions, $a = 4.71$ Å in our SIESTA calculations, is explicitly indicated.

Table 1. Atomic coordinates x, y, z (in units of a, see figure 2) of the main atoms in the upper layers of the surface for both reconstructions and their comparison with the available experimental data [19]. The zero vertical coordinate is shown in figure 2 by the dashed line drawn through some bulk atoms, the x and y axes are along the directions [1$\bar{1}$0] and [110], respectively, as shown in figure 2.

		4 × 2						c(8 × 2)					
Atom[a]		SIESTA			VASP			SIESTA			Experiment [19]		
In	1	2.000	0.506	−0.052	2.000	0.508	−0.051	2.000	0.500	−0.051	2.000	0.500	−0.051
In	2	0.000	1.000	−0.132	0.000	1.000	−0.127	0.000	1.000	−0.270	0.000	1.000	−0.295
In	3	0.000	0.000	−0.223	0.000	0.000	−0.206	0.000	0.000	−0.172	0.000	0.000	−0.203
In	4	0.876	0.000	−0.160	0.880	0.000	−0.146	0.889	0.000	−0.113	0.881	0.000	−0.159
In	5	0.885	1.000	−0.087	0.881	1.000	−0.085	0.887	1.000	−0.154	0.884	1.000	−0.162
Sb	6	0.514	0.483	−0.069	0.509	0.483	−0.063	0.528	0.509	−0.081	0.532	0.511	−0.106
Sb	7	1.496	0.000	−0.209	1.500	0.001	−0.196	1.493	−0.000	−0.200	1.485	0.000	−0.220
Sb	8	1.498	1.000	−0.202	1.499	1.000	−0.190	1.496	1.000	−0.205	1.493	1.000	−0.255
In	9	0.504	0.691	−0.478	0.504	0.690	−0.473	0.511	0.315	−0.502	0.516	0.315	−0.536
In	10	1.476	0.504	−0.466	1.476	0.503	−0.454	1.484	0.497	−0.469	1.483	0.500	−0.490

[a] Atomic numbers correspond to those in figure 2 and are the same as in [19].

The atomic positions for all symmetry unrelated atoms in the upper layer (in units of a, see figure 2) are given in table 1. Note the positions of atoms marked 9. These form a rectangle consisting of two dimers oriented in the [110] direction, with two In atoms each. These dimers are aligned with each other along the [1$\bar{1}$0] direction. Comparing the atomic positions obtained using the localized (SIESTA) and plane wave (VASP) basis sets, we see that the SIESTA results agree rather well with those of the VASP calculations: atomic positions deviate by no more than 0.07 Å. This confirms once again that the localized basis set used in SIESTA is appropriate.

The c(8 × 2) reconstruction is obtained by shifting positions of In-9 sublayer atoms along the [110] direction, as shown schematically in figure 3. The supercell consisting of two primitive cells as shown on the right in figure 2 (top and side views) was used in our calculations of this reconstruction. The relaxed structure of the c(8 × 2) reconstructed surface obtained using the same computational method and the SIESTA code are the detailed positions of the atoms in the upper layers, and their comparison with experimental ones obtained in diffraction experiments [19] are shown in table 1.

One can clearly see from the table and figure 2 that the point group of this surface is C_{2v}. A detailed analysis shows that the space group of the relaxed c(8 × 2) model is $c2mm$, the same one as obtained in the diffraction experiments [5]. If in the 4 × 2 reconstructed surface the rectangles formed by two In-9 dimers are perfectly aligned along the [1$\bar{1}$0] direction, in the c(8 × 2) reconstructed surface the positions of these appear to be shifted along the [110] direction in an alternating fashion creating a characteristic for this reconstruction body-centred pattern. If we consider now the atomic positions in detail (see table 1), we see that, indeed, the main difference between the two reconstructions is in the positions of the In-9 atoms; the lateral positions of other atoms change insignificantly, only

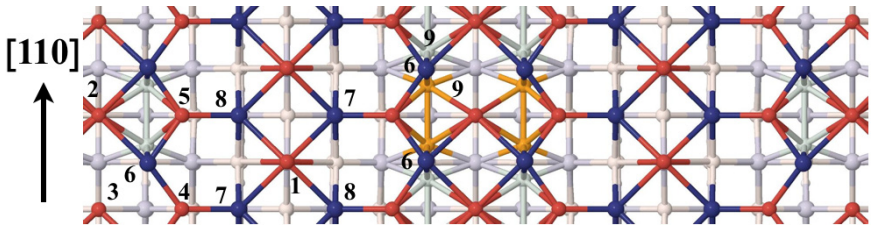

Figure 3. Schematics illustrating the difference between the 4 × 2 and c(8 × 2) reconstructions: the two colours show the two possible positions of the sublayer In-9 atoms (forming dimers) corresponding to the two reconstructions. Grey In-9 atoms form c(8 × 2) symmetry, gold ones correspond to the 4 × 2 reconstruction.

some deviations in their vertical position can be seen. The largest difference is observed for In-2 atom ($\Delta z = 0.138a = 0.65$ Å) which is shifted more inside the surface in the case of the c(8 × 2) reconstruction. In-3 and In-4 atoms move upwards respectively by 0.24 and 0.22 Å in the c(8 × 2) structure as compared with the $c(4 \times 2)$ one, while In-5 atoms move downwards by 0.32 Å. Note that, as a result, In-4 and In-5 atoms are at different heights of ≃0.19 Å in the c(8 × 2) reconstructed surface; in the experimental data these atoms' vertical positions are much closer. No significant changes in the positions of Sb and other In atoms were found. The obtained In–In distance between In-9 atoms in the dimer is found to be 2.97 Å, which is very close to the experimental value of 2.89 Å [5] (but note that our theoretical lattice constant is slightly larger). In fact our SIESTA geometry compares reasonably well (in units of a) with the diffraction data given in the same table. For all symmetry inequivalent ten atoms comprising the upper layer of this surface their lateral positions agree with experimental data reported in [5] (and table 1) better than $0.01a$ (around 0.05 Å). Their vertical positions do however deviate more from the experimental results, with the largest discrepancy of about $0.05a$ (about 0.24 Å) found for In-4 and Sb-8 atoms.

It follows from our calculations that both reconstructions are stable; moreover, they were found of practically the same stability: indeed, the total energies of the two supercells considered above for the 4 × 2 and c(8 × 2) reconstructions were found, within the precision of our calculations, to be the same. Since the two reconstructions can be obtained by shifting the sublayer In-9 atoms, and due to the high symmetry of the two reconstructions, one can consider the transition state separating the two. This would correspond to the middle position between the gold and grey coloured In-9 atoms of the two reconstructions, as shown in figure 3. By keeping the symmetry of the structure corresponding to these positions of the In atoms, we relaxed it and found that its energy is by 1.42 eV higher. Note that this is the energy per supercell, which is two times larger than the primitive cells in the two cases. Note that no vibrational analysis of the transition state was performed due to the expense of such a calculation; however, because of the nature of this state and the symmetry arguments, we believe it must be a saddle point. Hence, we conclude that the two reconstructions are separated by a very high energy barrier if the transition between the two reconstructions is assumed to happen in all unit cells at once (the barrier is proportional to the number of unit cells involved). Although

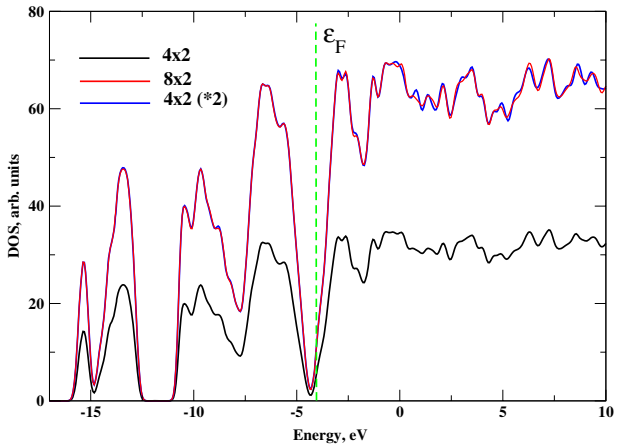

Figure 4. The total electronic DOS of the 4 × 2 (using the primitive unit cell, black line) and c(8 × 2) (using the cell shown in figure 2, red line) reconstructed InSb(001) surfaces. The blue line corresponds to the DOS of the 4 × 2 system with the same cell size as the c(8 × 2) system, i.e. multiplied by a factor of 2. The Fermi energy of the surface is specifically indicated by the (green) dashed line.

we do not consider here a possible mechanism for such a hypothetical transition, we note that a larger transition rate may be achieved if this transition happens locally in one or a small number of adjacent cells and then propagates across the surface, i.e. the whole transformation takes place after many steps moving from one cell to the other. We do not consider this process in this paper, however, as much larger supercells are necessary to verify whether this local transformation is stable. This analysis may also be relevant for understanding the structure of the low temperature phase, as mentioned in section 3.

Hence, our DFT calculations did not indicate the preference of the c(8 × 2) reconstruction, i.e. both reconstructions are equally probable on the surface. This is in contradiction to the observations which indicate that in all experiments reported here and previously [5, 19, 7, 6] the 4 × 2 reconstruction has never been observed, contrary to the InAs case [21]. It is not clear at the moment why this is so; we shall touch upon this point also in a later section 5.

4.2. Electronic properties

The electronic total densities of states (DOS) for the two reconstructions are shown in figure 4. These were calculated

using a histogram method from the Kohn–Sham energies calculated at a single $\mathbf{k} = 0$ point; we believe it is sufficient for our purposes due to rather large unit cells in the two systems. One can see that the two DOS have a very similar shape. Moreover, if the DOS of the 4×2 system is multiplied by a factor of 2, it becomes practically indistinguishable from the DOS obtained for the c(8×2) system. This means that the electronic structures of the two reconstructions are indeed very similar. Note that since the InSb has a very small band gap of 0.17 eV [20], this does not show up in our DFT calculations; as expected, the Fermi level falls within a deep dip in the DOS.

The similarity of the electronic structure for the two surface reconstructions is also evident in their calculated STM images. We show in the left panels of figure 1 the calculated STM images of the 8×2 reconstructed surface for both occupied (bias $V = -1.0$ V) and unoccupied (bias $V = 1.0$ V) states obtained using the 10 layer slab system. In the occupied states image one can clearly see bright lines of round features running in the [110] direction which are attributed to the In-1 atoms. Around these lines two considerably less bright round features are seen; one of them is attributed to a combination of Sb-7 and adjacent In-4 atoms, while the other is attributed to a combination of the Sb-8 and In-5 atoms; both features alternate along the [110] direction. Further, in the occupied states image right between the In-1 rows one can see rather bright features which appear at the positions of the Sb-6 atoms. Every nearest four such features form a rectangle. These rectangular groups are arranged along the [110] direction in the middle between the In-1 lines. They are shifted in adjacent rows by a (see the right panel of figure 2) in perfect correspondence with the dimerization of the In-9 atoms which lie underneath the Sb-6 atoms and are responsible for this reconstruction. In contrast, in the calculated occupied states STM image of the 4×2 surface (not shown) these features are perfectly aligned in each such row because of the alignment of the sublayer In-9 atoms, as was discussed in section 4.1. Both the bright lines and the rectangular features forming a brick-wall-like pattern agree perfectly with the occupied states experimental STM image (measured at the same bias voltage) shown in the left-upper panel of figure 1.

We have also calculated the STM images for higher bias voltages (not shown). Although the features between the bright lines, similarly to the experimental observations (see section 3), do look brighter at higher bias and there is no visible difference between the features associated with the Sb-6 atoms (see discussion above), so that the surface appears as 4×1 rather than as c(8×2), one may consider this agreement as accidental bearing in mind that the Tersoff–Hamann approximation is less reliable at higher bias voltages.

The STM image of the unoccupied states is given in the left-bottom panel of figure 1. The bright line of round features due to In-1 atoms is clearly visible here as well. However, the regions between these lines no longer consist of rectangular features as in the case of the occupied state image. Instead, oval dark features become immediately obvious, whose positions are shifted (also by a) in the adjacent rows in agreement with the c(8×2) reconstruction. The dark spots correspond to In-2 atoms which are placed quite deep inside the surface, see table 1. Two slightly brighter spots to the right and left of the dark spot are due to In-5 atoms. One can also see three round spots horizontally aligned above and below the dark ovals; each of these are due to a sequence of In-4, In-3 and In-4 atoms. One can see from table 1 that In-4 atoms are by 0.28 Å positioned higher than In-3 atoms, which explains the obtained contrast. Note that in the unoccupied states image of the 4×2 reconstruction all the same features are present; the only difference is that these are not shifted in the adjacent rows, otherwise, the image looks quite similar (not shown). The calculated unoccupied states image also agrees rather well with the experimental one reported above (see the right-bottom image in figure 1). Indeed, on both pictures we see parallel bright lines separated by a distance of $4a$, and between the lines there are short perpendicular lines which are offset by a in adjacent rows and separated by $2a$ within the rows. The oval dark features between the short lines in the theoretical image in the left-bottom panel of figure 1 correspond to dark regions between the short lines of the experimental image.

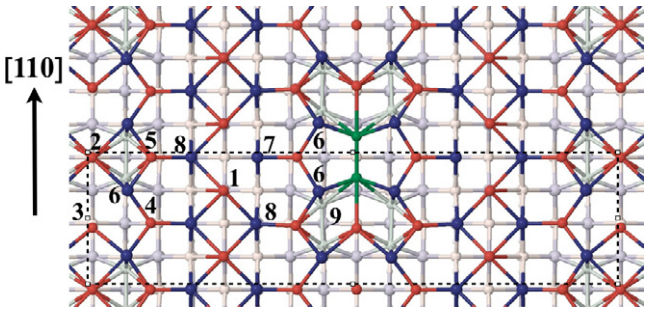

Figure 5. The top view of the 8×4 cell of a defective structure formed by an added In atom which forms a dimer with a sublayer In atom (both shown in green). The [110] direction and the 8×2 cell are indicated for convenience. The structure was relaxed using SIESTA. To help the comparison with the perfect c(8×2) surface shown in figure 2, some atoms of the upper layer have been numbered accordingly.

4.3. Top bilayer dimer defect

Kumpf *et al* [5, 19] also noted the possibility of some 'defective' sites in the top surface bilayer formed by an additional In atom bonding to In3 atom thereby creating an In–In dimer (marked 2d in [5, 19]). Although these dimers were found to be of relatively low population (28%) for InSb (however, they seem to be more abundant in the case of the GaAs(001) surface), we wanted to understand if these may be seen on the STM images of this surface. To check this point, we have modelled this defective system using a 8×4 unit cell. The top view of the relaxed (with SIESTA) structure is shown in figure 5, with the dimer In atoms marked as green. We find that this defective structure is stable and well localized, i.e. noticeable relaxation was only found for the neighbouring surface atoms. We did not study the diffusion of this sublayer In dimer.

The corresponding STM images of the defective structure, for both occupied and unoccupied states (and the bias voltage of ± 1.0 V), are shown in figure 6. As a result, the dimer appearance in the occupied states STM image, shown in the left

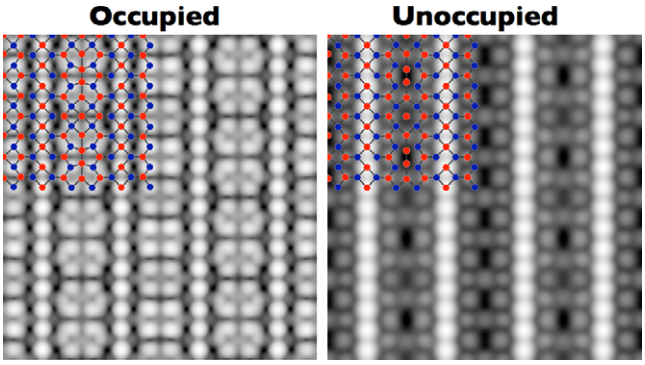

Figure 6. Calculated STM images of the dimer defect of figure 5: left—occupied states ($V = -1.0$ V); right—unoccupied states ($V = 1.0$ V). In each case eight 8×4 cells are shown. Two cells of the upper layer of atoms are superimposed on the images for convenience.

panel of figure 6, is almost the same as that of the rectangular feature of the dimer-free surface shown previously in figure 3. Although some changes are noticeable in the unoccupied states image in the contrast of the oval dark spot, these are small. This means that it is highly doubtful that these sublayer dimers can be recognizable in the observed STM images.

5. Discussion and conclusions

The relaxed geometry of the c(8×2) reconstructed surface agrees rather well with the x-ray diffraction data due to Kumpf *et al* [5, 19]. The calculated characteristic length $a = 4.709$ Å in the system (see figure 2) compares well with that observed experimentally, $a = 4.5816$ Å. Therefore, we clearly demonstrate that the structure of the InSb(001) surface proposed by Kumpf *et al* does correspond to a stable structure. However, our calculations failed to demonstrate a significant difference in stability between this c(8×2) reconstruction and the 4×2 one which has not yet been observed for this surface.

We also find an excellent agreement between the calculated and experimentally observed room temperature STM images of the c(8×2) reconstructed surface corresponding to the occupied and unoccupied states, reported in figure 1. Indeed, in both cases one can clearly see lines of bright features running along the [110] bulk direction, with the lines separated from each other by the same distance of $4a$ as in the experimental image. The distance between the bright features along the lines, as follows from our calculations, corresponds to a. Although in our experimental images presented here the bright lines were not resolved, it was found in earlier RT experiments [6], that they indeed consist of bright spots separated by the same distance of a. The major characteristic details found between the lines in both types of theoretical images (occupied and unoccupied) also agree well the corresponding experimental ones: we see either rectangular (the $V = -1.0$ V occupied states image) or linear (the $V = +1.5$ V unoccupied states image) bright features running in the [110] direction between the bright lines and offset in the adjacent rows by a. It is exactly these features between the bright lines which indicate clearly on the c(8×2) reconstruction of the InSb(001) surface.

Such a remarkable agreement between the calculated and measured STM images is extremely encouraging considering the fact that the approximate Tersoff–Hamann method [15] was used here for calculating the STM images; this does not take account of the imaging conditions (e.g. tip structure). Overall, our results do seem to confirm the Kumpf *et al* model of the InSb(001) surface. We have also demonstrated by a direct calculation that the sublayer In dimer defective structure, proposed by Kumpf *et al*, although stable, is unlikely to be distinguished in STM images from the features of the perfect surface.

In spite of this agreement, our analysis cannot be complete and the structure we obtained definite, as in our modelling we did not take into account the observed partial populations of various sites in x-ray diffraction experiments [5, 19], most importantly, of the In1 site which was found to be nearly half populated (at 57%). At the same time, the Kumpf *et al* model, and hence our calculations, do not explain the observed low temperature (LT) phase of this surface [6], in which the symmetry is clearly lower. Indeed, a number of new features were observed at 77 K, such as tilting of pairs of bright features, 'defect' features of various shapes which change their positions along the lines of bright features almost at random, etc. These new features effectively create a superstructure on top of the c(8×2) reconstruction leading to a noticeable deviation from the rather high symmetry observed at RT. A possible random distribution of the sublayer In dimer defects cannot explain the observed LT features, as is clear from our results reported in section 4.3. Partial population of In-1 sites (and hence a significant population of surface vacancies) may be a definite factor explaining the symmetry lowering observed at LT. Indeed, if there are instabilities on the surface (e.g. vacancies jumping between nearest lattice sites), then the 'frozen' surface at LT may appear of lower symmetry than at the RT when all possible positions of the vacancies are averaged over (e.g. due to possibly fast diffusion of the vacancies). Partial populations of the lattice sites may also be the reason for making the 4×2 reconstruction, never observed experimentally for the InSb(001) surface, to be less favourable than the c(8×2) one. The work on identifying possible instabilities on this fascinating surface are currently in progress.

Summarizing, in this paper we performed a joint experimental (at RT) and theoretical study of the InSb(001) surface. For the first time we considered, using an *ab initio* DFT method, the c(8×2) reconstruction of this surface. We find that the ζ-model due to Lee *et al* [4] and Kumpf *et al* [5, 19] does correspond to a stable structure. According to this model, sublayer In-9 atoms tend to approach each other forming dimers, and this particular relaxation results in a characteristic c(8×2) pattern. We have also found that the sublayer In-9 atoms can occupy several alternative positions along the [110] direction leading to either 4×2 or c(8×2) reconstructions with practically no change in the total energy of the system; however, the barrier between the two reconstructions was found to be considerable. The calculated STM images of the c(8×2) reconstruction agree remarkably well with the negative and positive bias experimental STM

images, both reported here and previously [6]. No 4 × 2 reconstruction of this surface has so far been observed.

We believe that this paper will stimulate further work aimed at understanding the complex structure of the InSb(001) surface.

Acknowledgments

Jiangping He and Dawid Toton would like to acknowledge the financial support from the European Integrated project PicoInside (contract No. FGP-015847); Dawid would also like to acknowledge a grant from the Thomas Young Centre which made his visit to London possible. Computer time allocation on the HPCx and HECToR UK National facilities via the Material Chemistry consortium is greatly appreciated. The experimental part of this work has been supported by the Polish Ministry of Science and Higher Education under contract no. 0357/B/H03/2009/36. Szymon Godlewski and Marek Szymonski acknowledge the support from the Polish Foundation for Science (Contract for Subsidy 11/2007-2010). The authors acknowledge support from the 7th Framework Programme 'NanoICT', contract no. 216165.

References

[1] Goryl G, Godlewski S, Kolodziej J J and Szymonski M 2008 *Nanotechnology* **19** 185708
[2] Tekiel A, Goryl M and Szymonski M 2007 *Nanotechnology* **18** 475707
[3] Schmidt W G 2002 *Appl. Phys.* A **75** 89
[4] Lee S-H, Moritz W and Scheffler M 2000 *Phys. Rev. Lett.* **85** 3890
[5] Kumpf C *et al* 2001 *Phys. Rev. Lett.* **86** 3586
[6] Goryl G *et al* 2007 *Surf. Sci.* **601** 3605
[7] Kolodziej J J *et al* 2006 *Appl. Surf. Sci.* **252** 7614
[8] Soler J M *et al* 2002 *J. Phys.: Condens. Matter* **14** 2745
[9] Perdew J, Burke K and Ernzerhof M 1996 *Phys. Rev. Lett.* **77** 3865
[10] Harrison W A 1980 *Electronic Structure and the Properties of Solids* (San Francisco: Freeman)
[11] Madelung O, Schulz M and Weiss H (ed) 1982 *Numerical Data and Functional Relationships in Science and Technology* (*New Series, Group III*) vol 17a (Berlin: Springer)
[12] Kresse G and Furthmüller J 1996 *Comput. Mater. Sci.* **6** 15
[13] Kresse G and Furthmüller J 1996 *Phys. Rev.* B **54** 11169
[14] Blöchl P E 1994 *Phys. Rev.* B **50** 17953
[15] Tersoff J and Hamann D R 1985 *Phys. Rev.* B **31** 805
[16] Schweitzer M, Leibsle F, Jones T, McConville C and Richardson N 1993 *Surf. Sci.* **280** 63
[17] Varekamp P R, Björkqvist M, Göthelid M and Karlsson U O 1996 *Surf. Sci.* **350** L221
[18] Davis A A *et al* 1999 *Appl. Phys. Lett.* **75** 1938
[19] Kumpf C *et al* 2001 *Phys. Rev.* B **64** 075307
[20] Littler C L and Seiler D G 1985 *Appl. Phys. Lett.* **46** 986
[21] Kendrick C, LeLay G and Kahn A 1996 *Phys. Rev.* B **54** 17877